Developing of biophysical food for monitoring postharvest supply chains for avocado and potato and deploying of biophysical apple

Lingxin You[1,2], Seraina Schudel[1], Thijs Defraeye[1*]

[1] *Empa, Swiss Federal Laboratories for Material Science and Technology, Laboratory for Biomimetic Membranes and Textiles, Lerchenfeldstrasse 5, CH-9014 St. Gallen, Switzerland*

[2] *ETH Zurich, Department of Health Science and Technology, Universitätstrasse 2, CH-8092 Zurich, Switzerland*

** Corresponding author, thijs.defraeye@empa.ch*

Abstract

Horticultural products are prone to high postharvest losses due to their perishability and susceptibility to drivers for food decay, including temperature. A narrow temperature window must typically be maintained to prevent accelerated decay and, at the same time, thermal damage, such as chilling injury. Food simulators or so-called biophysical food help monitor postharvest supply chains, preventing temperature abuse in the cold chain, and optimizing refrigerated transport and storage. This biophysical food for fruit and vegetables needs to be tailored for each commodity or cultivar to consider different physical properties influencing their thermal response. We developed new biophysical food for two sizes of both avocado (cv. 'Hass') and potato (cv. 'Kufir Jyoti' and 'Agria'). The shell design and filling were adapted to mimic the specific characteristics of the real products. Integrated sensors were log core and surface temperature. Furthermore, we optimized the production steps of our existing biophysical food prototype for apples (cv. 'Braeburn') and deployed them in a cold storage facility in India. Thereby our biophysical apple was used to map the thermal distribution inside a cooling unit. By mimicking the real commodities' thermal response via biophysical food, we gain complementary insights compared to only monitoring air temperature. Our plug-and-play biophysical food can be stored with real food, particularly to sense conditions in hard-to-reach locations. These biophysical food temperature data will help improve cold chain operations to achieve optimal and homogenous cooling and decrease postharvest losses.

Keywords: food simulator, temperature monitoring, food loss, cold chain, sensor, fruit thermal response

1 INTRODUCTION

Fruit and vegetables have always been an essential component of the human diet because they contain various essential nutrients such as vitamins, dietary fiber, potassium, and folate (Pennington & Fisher, 2010). However, despite several years of postharvest technology development, estimated losses and fruit and vegetable waste can still amount to 40% every year, including 25%-30% from farm to retailer (FAO, 2013, 2015). The deterioration of fruit and vegetables depends highly on the product's environmental conditions, such as temperature, humidity, and the concentration of surrounding gases (e.g., CO_2, O_2, and C_2H_4). Temperature is typically the most crucial factor influencing the product's shelf life among these parameters. Monitoring temperature within cold chains, especially during storage and transportation operations, can help to identify weak points in the cold chain. By solving these, we can considerably improve the quality retention of fresh produce in order to help decrease food losses.

Few studies have been conducted about novel fresh produce simulators monitoring temperature, humidity, or respiration (de Mello Vasconcelos, de Campos Ferreira, de Castro Silva, Teruel Mederos, & de Freitas, 2019; Geyer et al., 2018; Hübert & Lang, 2012; Keshri et al., 2020). A fruit simulator sensor device recently described by (Defraeye et al., 2017) was developed to monitor and analyze product temperature more realistically in order to improve storage and transport conditions in the cold chain. We further refer to this simulator as biophysical food of a fresh product of interest. The concept of biophysical food was initially designed for apples and later extended to mango products (Defraeye et al., 2019, 2017). Thereby, the prototype is composed of a thin plastic shell that mimics the exterior size and shape of the commodity. Its shell is filled with a thermal filling that has similar thermal properties to a real fresh product. This filling consists of a water-carbohydrate mixture including expanded polystyrene (EPS) particles that mimic the intercellular air space. In this way, this food simulator reacts thermally similar to the real product. Two iButton® temperature sensors (Maxim Integrated Products, USA) are integrated at the surface and center to obtain the surface and core temperature.

Nowadays, various sensor logger devices are available for temperature monitoring along the supply chain (Onwude et al., 2020). Different devices with sensor probes for assessing pulp temperature are available in the market. Examples are FlashLink® Reusable USB Data Logger (DeltaTrak Inc., USA) or TempTale® Ultra (Sensitech Inc. USA). Nevertheless, they have a drawback due to their destructive measurement by puncturing the fruit skin and possibly leading to an entry for pathogens. On the other hand, our biophysical food can directly be packed with fresh produce, and the integrated sensor logs the pulp temperature in a non-destructive way. This is achieved as the biophysical food's design mimics the thermal response of the product of interest throughout the cold chain.

Biophysical food was developed to overcome the current limitations of temperature monitoring in fresh commodities' postharvest supply chains. The easy installation also enables putting them in multiple locations within a cargo or a cooling chamber to identify temperature heterogeneities associated with quality variations and decay. Other than in most supply chains, where only a segment is monitored, the biophysical food can be stored together with the products from harvest to retail due to easy handling and long battery lifetime enabling continuous monitoring (Shoji, Schudel, Onwude, Shrivastava, & Defraeye, 2022). In addition, it is a stand-alone unit without cabling, which means there is no effect on the airflow field and cooling behavior of the surrounding produce (Defraeye et al., 2017). However, the design of this kind of biophysical food needs to be adapted for different commodities due to varying physical properties and the corresponding thermal response. For example, the concept adapted for mango provides two filling cavities with different chemical compositions, mimicking both the flesh and stone properties (Defraeye et al., 2019). To further explore the potential of biophysical food, we need to develop it for additional commodities, optimize the manufacturing process to scale up straightforwardly, and deploy it in real supply chains.

In this study, we tackled these challenges. We first optimized the manufacturing process of the current biophysical apple. We added anti-fungi material to the filling and applied proper color and coating to the shells, which are essential for further commercial use of the biophysical food. Then, to increase the variety of biophysical food for different applying situations, we designed and validated two sizes of avocado (cultivar (cv.). 'Hass' small/large) and potato (cv. 'Agria' and 'Kufir Jyoti'). Finally, to investigate the performance of biophysical food in the field, we sent our apple prototypes to our collaborators in India to test part of the actual cold chains. Then, we analyzed the cooling and storage temperature data to reveal the heterogeneity in the cooling unit. By using biophysical food in fresh produce supply chains, complementary insight into temperature variation can be obtained. These data will help improve cold-chain operations, consequently reducing food losses.

2 MATERIALS AND METHODS

2.1 Design of biophysical food for avocado and potato

2.1.1 Prototypes shape information

The cultivar 'Hass' was chosen for the avocado prototype, and its size characteristics that were required to build the 3D model were obtained from bought avocados (Migros supermarket, Switzerland). Based on the measurements, we found a wide variety for the size of this cultivar. Typically, the size variation of avocados is influenced by many factors, including seasonality and product origin. Therefore, we decided to have two versions of biophysical avocado representing a small and large 'Hass' avocado deployed for different product size classes. Similarly, we designed small and large versions of potato products. For this, we selected the cultivars 'Kufir Jyoti' (small) and 'Agria' (large), which are both widely produced and consumed in Asia (India) and Europe, respectively. A reason for the choice was that one of our collaborators is located in India, and the 'Kufir Jyoti' was of specific interest to that market. However, in the validation part, we used small potatoes of a similar size as cv. 'Kufir Jyoti' since it was not available (section 2.3).

X-ray technology can be used to accurately obtain the shape of the commodity for the prototype's shell, which was previously described by (Defraeye et al., 2017). In this study, we obtained the physical size and shape parameters either from measurements or from literature for avocado and potato, respectively (Table 2.1, Table S1, Table S2). We then used Rhino 7 software (McNeel Europe S.L., Spain) to build the exterior shape.

Table 2.1 Dimension and density of small and large avocado and potato.

	Small avocado[a]		Large avocado[a]		Small potato[b]	Large potato[c]
	Whole avocado	Seed	Whole avocado	Seed		
Length [mm]	90.87	39.11	97.95	42.70	57.68	95.14
Width [mm]	58.47	35.49	70.64	36.32	37.77	63.00
Density [g/cm^3]	1.02	1.18	1.02	1.18	1.10	1.10

[a] Length and width were measured using a Vernier scale. Density was calculated by "ρ = m/V" (Volume measured by displacement method) and adjusted based on (Valente, Chambarel, Cordonnier, & Pumborios, 1996). [b] (D. K. Singh, Goswamin, & Chourasia, 2006). [c] (Ahangarnezhad, Najafi, & Jahanbakhshi, 2019).

2.1.2 Shell model development

The main structure of the shell was built in Rhino 7 using curve tools with interpolating points, 2D and 3D geometrical tools, as well as surface tools like revolve. Combining trim, join, and offset surface functions, a shell with a 2 mm thickness wall was obtained. For potatoes, we used an organic shape shell for which the first step was varied. Using the loft function, the outer structure was built by connecting four different shape curves. The final 3D models for a biophysical avocado and a biophysical potato are shown in Figure 2.1. By selective laser sintering polyamide (FDA-approved as 'food-safe'), 3D prototypes of different products were printed (Materialise NV, Belgium).

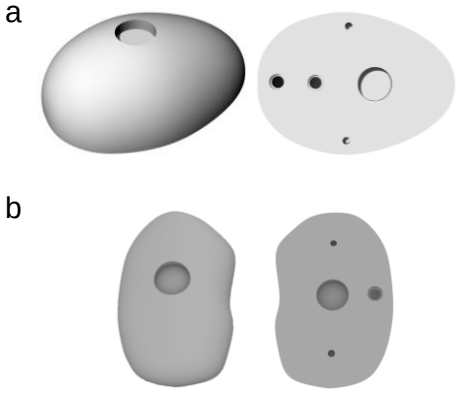

Figure 2.1. 3D printed models of (a) a biophysical avocado and (b) a biophysical potato designed with Rhino 7.

2.2 Optimization of the current design and manufacturing steps

2.2.1 Gel filling

Gel component

Horticultural products are typically composed of mainly water and carbohydrates, whereas their ratio varies between different species (ASHRAE Research, 2018). This composition and its air porosity (through the air in the intercellular spaces) consequently

lead to a specific density, thermal capacity, and thermal conductivity for each species. To mimic the composition of apple, avocado, and potato in the biophysical food prototypes, we used water, sugar, agar, and EPS particles (diameter 0.5-1.5 mm) as substitutes. The procedure was previously described in (Defraeye et al., 2017), but we optimized it in this study to reduce manual labor as this is essential for producing these novel products in larger quantities. Agar enables the liquid solution to become a solid gel that keeps the EPS particles suspended. The real apple, avocado, and potato compositions are listed in Table 2.2, and the corresponding selected biophysical product gel compositions that we manufactured are shown in Table 2.3.

The specific manufacturing parameters were adjusted depending on different compositions for each commodity, whereas the gel for all biophysical food was prepared similarly. Therefore, sugar and agar were dissolved in water in a glass bottle and then heated in a microwave until all the components were fully dissolved. Subsequently, the solution was cooled down in a controlled manner in a water bath to a specific temperature (Table 2.4). Then, the EPS particles were added to the solution and mixed until they were homogeneously distributed. Finally, the density of the finished prototype was calculated by dividing the measured weight by the volume of the biophysical food (obtained from Rhino). We set a density difference of 5.0% to be acceptable compared to the real commodities.

Table 2.2 Composition of real apple, avocado, and potato.

Real Product		Water [%][a]	Carbohydrates [%][a]	Protein [%][a]	Fat [%][a]	Ash [%][a]	Porosity [%][b]
Apple[c]		83.93	15.25	0.19	0.36	0.26	13.00
Avocado[d]	*seed*	15.10	49.03	15.55	17.90	2.26	7.90
	pulp	64.50	7.80	2.20	24.00	1.50	1.90
Potato[e]		77.00	20.13	1.87	0.10	0.90	0

[a] Mass fraction. [b] Volume faction. [c] (ASHRAE Research, 2018). [d] (Clark, White, Jordan, & Woolf, 2007; Dreher & Davenport, 2013; Ejiofor, Ezeagu, Ayoola, & Umera, 2018; Kader & Yahia, 2011; Olaeta, Schwartz, Undurraga, & Contreas, 2007; Salazar-López et al., 2020). [e] (FAO, 2008; Puttongsiri, Choosakul, & Sakulwilaingam, 2012; Ramezani & Aminlari, 2004; D. K. Singh et al., 2006; F. Singh, Katiyar, & Singh, 2015; Sukhpreet & Poonam, 2014; Yang, Achaerandio, & Pujolà, 2016).

Table 2.3 Gel composition of biophysical apple, avocado, and potato.

Biophysical Product		Water [%][a]	Sugar [%][a]	Agar [%][a]	EPS [%][b]
Apple		83.93	15.07	1.00	13.00
Avocado	*seed*	17.00	81.50	1.50	9.00
	pulp	70.00	25.00	5.00	7.00
Potato		77.00	21.00	2.00	0

[a] Mass fraction. [b] Volume faction.

Table 2.4 Water bath temperature for cooling different biophysical food gel fillings.

	Apple	Avocado pulp	Avocado seed	Potato
Temperature [°C]	45	80	80	50

pH adjustment

We adjusted the gel's pH to prevent fungal growth in the gel filling, an observed issue of the previous prototypes. Experiments were performed to decrease pH using citric acid, tested by litmus paper. It was determined that adding 3 mL 0.028 g/mL citric acid solution to a 280 mL mixture solution (before gelling) reached a pH of 3 (n=3), which is enough to inhibit common fungal growth (Rousk et al., 2010). With this amount of citric acid, the impact of its concentration on the components in the gel was negligible.

Filling

In **Error! Reference source not found.**, the thermal properties of the gel mixture were calculated based on (Defraeye et al., 2017) using the values in Table 2.2 and Table 2.3.

Table 2.5 Thermal properties for real and biophysical avocado seed and pulp and potato.

	Density [kg/m^3]	Specific heat [J/kg·K]	Thermal conductivity [W/m·K]
Real avocado seed	1178	2103	0.246
Biophysical avocado seed	1266	2018	0.260
Difference *seed*	7.4%	4.0%	5.8%
Real avocado pulp	1000	3332	0.459
Biophysical avocado pulp	1044	3366	0.446
Difference *pulp*	4.4%	1.0%	2.7%
Real potato	1089	3549	0.518
Biophysical potato	1090	3544	0.517
Difference	0.1%	0.1%	0.1%

2.2.2 Food-safe coating

The biophysical food should be viable to be in contact with food. Therefore we designed the shell for this purpose. For the initial biophysical apple and small biophysical avocado, we used blue spray paint to color the whole fruit. Later for the large biophysical avocado and both versions of the biophysical potatoes, the manufacturer performed the coloring directly after the 3D printed polyamide shell (Materialise NV, Belgium). Finally, a food-grade lacquer (I AM CREATIVE®, MAREIN AG, Switzerland) was applied to cover the whole product homogeneously.

2.2.3 Temperature sensors

The iButton® (Maxim Integrated Products, USA), wireless, small (diameter 17 mm, thickness 6 mm), and robust sensors, were fixed separately to the surface and center of biophysical food by double-sided adhesive pads. Thermochron type DS1922L (8kB memory @ 8bit, resolution 0.0625 °C, accuracy ±0.5 °C, from -40 °C to +85 °C, sampling rate from 1 s up to 273 h) and DS1921G (2kB memory @ 2bit, resolution 0.5 °C, accuracy ±1 °C, from -40 °C to +85 °C, sampling rate from 1 min up to 255 min) were used in this study.

2.3 Validation: Cooling experiments on biophysical food versus real commodities

We conducted cooling experiments to validate the thermal response of the biophysical food by testing them together with similar-sized real commodities for avocado and potato. Therefore, two cooling chambers (BINDER KB400, 1.90 kW, 400 L; ESPEC Corp., 0.06 kW, 312 L) were used. Temperature sensors with probes (Ecolog TN2, ELPRO-BUCHS AG, Switzerland, resolution 0.1°C, accuracy ±0.4°C; Tinytag Talk2, Gemini Data Loggers Ltd., UK, resolution 0.05°C, accuracy ±0.01°C) were used for core temperature monitoring of the real avocado and potato. Hygrothermal air conditions around the samples were monitored by a separate gadget (SHT4x Smart Gadget, Sensirion AG, Switzerland, resolution 0.01°C, accuracy ±0.2°C). The following software was used to set up and read out the sensors: elproLOG ANALYZE and Tinytag Explore. The sensor probes were inserted into the fresh food, and their wires were fixed by tape to prevent movement. OneWireViewer (Maxim Integrated Products, USA) software was used to set up the iButton sensors (DS1922L or DS1921G), which were integrated into biophysical food. Finally, MyAmbience APP was used to set up SHT4x Smart Gadget. The interval of recording was set as 1 minute for all the sensors. All samples (n=7 of real commodities plus one biophysical food) and sensors were put in a 25°C chamber to reach the same initial temperature and subsequently put into a second chamber with 5°C or 10°C for avocado and potato, respectively. After each test, sensors data was read out by the corresponding software, and the cooling curves were analyzed. In addition, the half cooling time (HCT) and seven-eighth cooling time (SECT) were calculated and compared as described in (Wu & Defraeye, 2018). For example, the avocado was cooled down from 25°C to 5°C as this is the optimum storage temperature for 'Hass' avocado (Dixon, Smith, Elmsly, Industry, & Box, 2004). The half cooling temperature was 15°C, while the seven-eighth cooling temperature was 7.5°C. The respective cooling time was obtained from the temperature curves.

2.4 Field experiments for deploying biophysical apple

To test our apple prototypes in real postharvest supply chains, three optimized biophysical apples (section 3.1) were sent to our collaborator (Coolcrop Technologies Pvt. Ltd., India), a company that facilitates cold storage units for small and marginal farmers. This deployment aimed to obtain sensor data from an actual supply chain and gather the user experience of the biophysical food in the field. In particular, we investigated the postharvest cooling and storage of apples before they are transported and sold at the market. The test location was in Himachal Pradesh. The apple cultivar was Royal Delicious, harvested in November, and stored around 4-5°C for four months. Although the biophysical food was produced for Braeburn apple, Royal Delicious has a similar average size and weight as that cultivar (Kumar & Singh, 2020; Mpelasoka, Behboudian, & Ganesh, 2001). The monitoring was conducted after harvest and a second time, after a month of storage, when the cool unit was filled.

In the first experiment (during harvest), two biophysical apples were stored in a cooling unit, where the first one was put in the top crate (on top of the apples) near the evaporator. The second biophysical apple was placed in the top crate (on top of the apples) near the center of the room. In the second trial, one biophysical apple was put in the middle crate (on top of the apples) on the opposite end of the evaporator near the door. The second biophysical apple was located in the top crate near the evaporator in the right corner. After the monitoring, the iButton sensors (DS1921G) data were read out and plotted.

3 RESULTS AND DISCUSSION

3.1 Optimizing the biophysical apple design and manufacturing

We evaluated different optimizations of the current design and manufacturing process of the first biophysical prototype previously developed in our laboratory for apple (Defraeye et al., 2017). The aim was also to improve the protocol (e.g., by minimizing manual labor) to enhance the production scalability of these biophysical foods. Firstly, the objective was to enhance the homogeneity of the distributed EPS particles in the filling mixture. Therefore, we identified the exact gelling point of the mixture and defined the temperature of 40°C at which the solution needed to be mixed with EPS particles. This adjustment in the protocol (section 2.2.1) will prevent the EPS particle from floating and accumulating at the filling solution's surface, which otherwise would occur during mixing at too high temperatures. Additionally, uniform cooling of the gel is essential to ensure a homogeneous distribution of the EPS particles before the shell filling step. Previously, this was done by gently shaking the gel mixture container. Nevertheless, using the water bath in this study enables the gel to cool more uniformly. Furthermore, we could avoid over-shaking of the filling mixture, which undesirably can lead to the inclusion of air and, by this, alteration of the porosity.

As a next step, we focused on the long-term preservation and prevention of mold growth in the filling gel. This was initiated as we sporadically observed contamination of stored gel test tubes. Fungal growth can be inhibited by both increasing (pH>9) and decreasing (pH<5) the mixture solution's pH (Rousk et al., 2010). Due to its low cost, required concentration, and easy availability, we chose citric acid as an additive for pH reduction (Hassan, Sand, & El-Kadi, 2012; Shokri, 2011). This method was also appropriate as EPS is chemically relatively inert and resistant to breakdown by acids ensuring the stability of the gel filling (Ferrándiz-Mas & García-Alcocel, 2013). Another way to suppress microbial growth could be to sterilize the gel mixture with high-temperature treatment. However, this was unsuitable as EPS is not resistant to a temperature above 100°C (Hajduković, Knez, Knez, & Kolšek, 2017). Another efficient possibility to be further explored could be the addition of anti-fungal materials, such as chitosan (Fang, Li, & Shih, 1994). Furthermore, long-term experiments to prove this preservation method and ensure the product's service life of the desired 4-7 years are still pending.

In the following step, we optimized the coloring and coating of the biophysical apple. Thereby, we not only changed the color from red to blue, which is easier recognized when used with real apples, but also applied a food-grade lacquer on the surface. Compared to the previous design, this added step ensures that the biophysical products can be stored together with real food.

Finally, we manufactured several biophysical apples using the improved protocol. We compared their density to the average density of real apples (0.925 g/cm^3) (ASHRAE Research, 2018), which is directly related to their thermal-physical response. These differences were acceptable since they were below 5.0% (between 0.7% and 3.8%). Three of these "optimized" biophysical apples (Figure 3.1) were sent and deployed in an apple cold chain in India, which is further described in section 3.4.

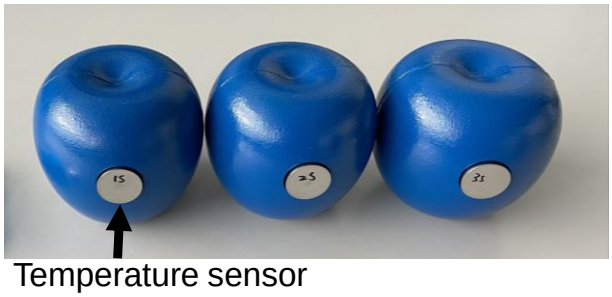

Figure 3.1 Three optimized biophysical apples that were sent and deployed in an apple supply chain in India.

3.2 Development of new biophysical food for avocado and potato

Firstly, we designed the shell structure for both avocado (cv. 'Hass', small and large) and potato (cv. 'Kufir Jyoti', small; 'Agria', large), where the details are described in section 2.1.2. The sectional views of both large prototypes are shown in Figure 3.2, displaying a polyamide shell providing the frame structure with cavities for thermal fillings. Since the avocado seed and pulp have different compositions, two cavities were designed for different corresponding gel fillings. The calculated differences of thermal properties (i.e., thermal conductivity, specific heat capacity) between the biophysical avocado gel fillings and real avocado were for all variables (seed and pulp) below 8%. Despite that any difference to the real species decreases the accuracy of the mimicked thermal response, these thermal fillings still come much closer to the real product than that of other food simulators for which often only a polymer shell is used (e.g., specific heat capacity difference to real fruit >70%) (Defraeye et al., 2017). For potatoes, the calculated difference for thermal properties was for all values below 0.2%. The agreement is much better due to the absence of fat, which could not be matched precisely with the current ingredients for the biophysical avocado.

The preparation of the gel filling and injection to the shells for the biophysical avocado differed from the apple prototype due to the high-temperature solidification and high viscosity of gel fillings. This was the case because the high sugar concentration led to difficulties during the shell filling step. On the other hand, the advantage of this filling mixture was that the EPS particles could easier be homogeneously distributed. An improvement from the small avocado (first prototype) to the large one was that the shell

coloring was already performed by the manufacturer of the 3D printing shell (Materialise NV, Belgium). This accelerated our manufacturing process and increased the stability of the color. The new version of the biophysical avocado was yellow (Figure 3.3 a,b). This appearance made it more prominent for storage with real avocados. The colors chosen for small and large biophysical potatoes were purple and red, respectively (Figure 3.3 c,d).

Finally, the calculated densities of both biophysical avocados were acceptable as they were in the same range as real avocados, with differences between 0.02% and 2.8%. Similarly, the density differences of the manufactured large potato prototypes were between 1.8% and 2.9% compared to reference values obtained from real potatoes. The measured density difference between small biophysical and real potatoes was between 4.9% and 5.9%. This number was still in the acceptable range, however, higher than in the larger prototype. A reason could be that the relative ratio of shell to filling is much higher in the small version, which could lower the density of the biophysical products since the polyamide shell has a smaller density.

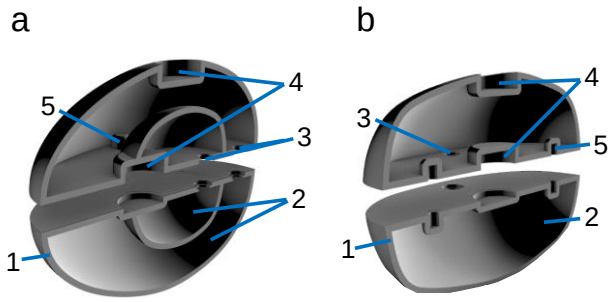

Figure 3.2. 3D model of (a) a large biophysical avocado and (b) a large biophysical potato designed with Rhino 7 software. 1: Rapid-prototyped polyamide shell; 2: Cavities for thermal filling; 3: Holes for filling; 4: Space for temperature sensors; 5: Magnets for connecting the two parts.

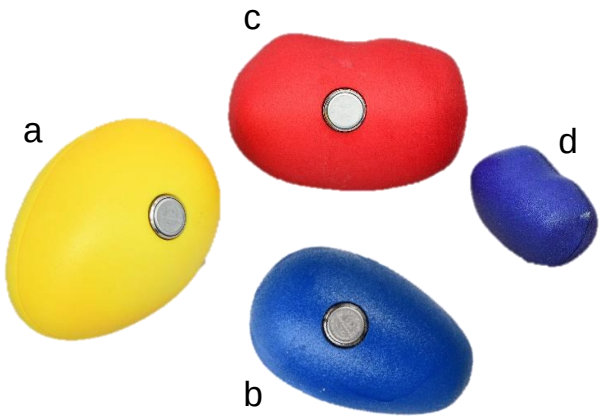

Figure 3.3. Prototypes for (a) large and (b) small biophysical avocado, and (c) large and (d) small biophysical potato.

3.3 Validation of the biophysical avocado and potato in the cooling process

3.3.1 Avocado

We performed cooling experiments to investigate whether the biophysical avocado captures real avocado's thermal response. Thereby, we compared data from sensors with probes inserted into real avocados for monitoring pulp temperature with the biophysical avocado's core sensor data. Subsequently, we calculated the half-cooling (HCT) and seven-eighths cooling (SECT) times that are typically applied in commercial cooling operations of fruit and vegetables (Defraeye et al., 2019; Wu & Defraeye, 2018). Both cooling curves of the real and biophysical avocado and the respective HCT and SECT are presented in the following (**Error! Reference source not found.**, Table 3.1).

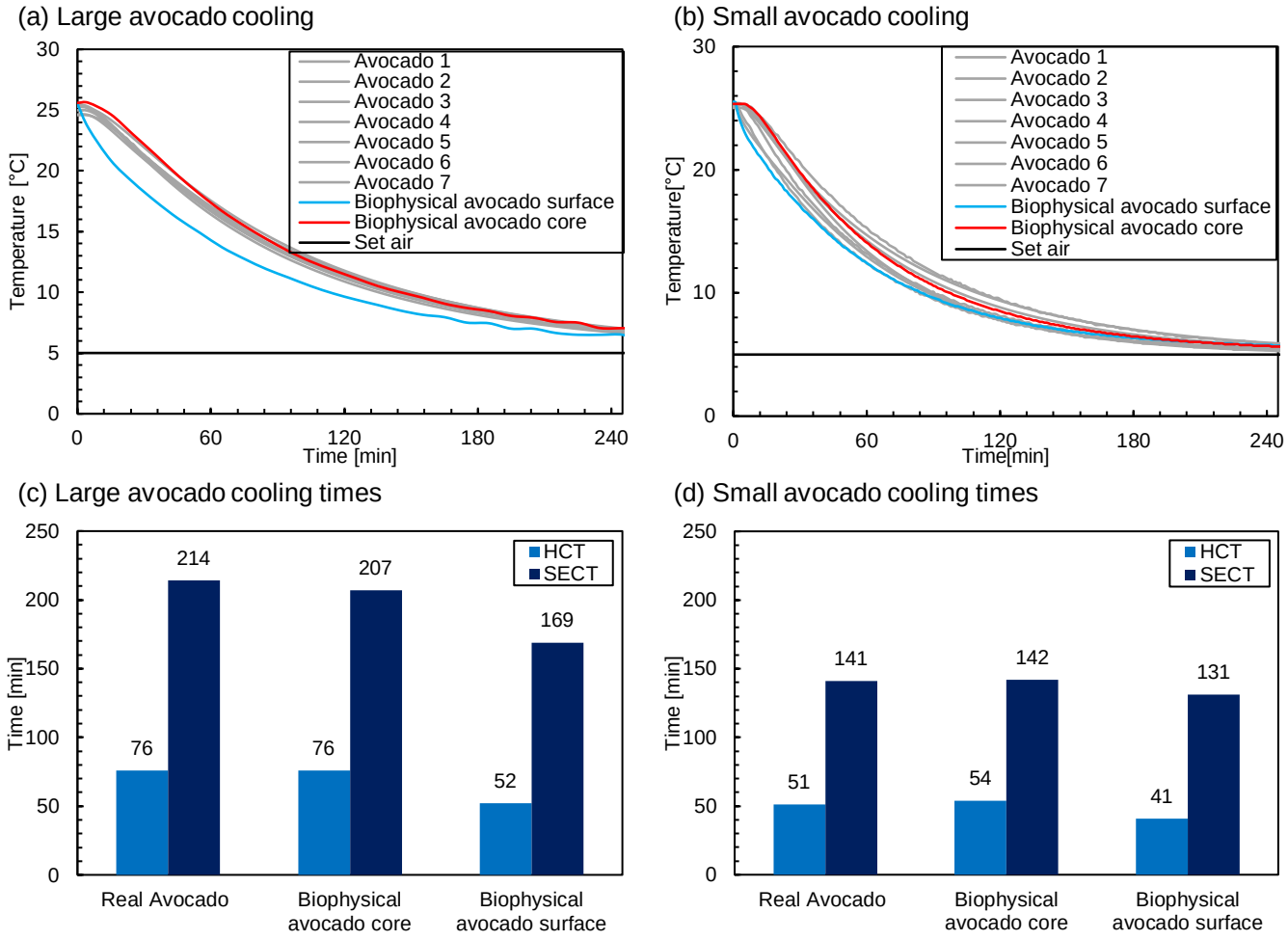

Figure 3.4. Time-dependent temperature change measured during cooling for (a) large and (b) small biophysical avocados together with real fruits. Monitored temperature for biophysical avocado surface (blue), biophysical avocado core (red), and core of the real avocados (grey), the chamber set temperature is indicated (black). Measured HCT and SECT of (c) large and (d) small versions of both real (n=7) and biophysical (n=1) when cooling from 25°C to 5°C.

Table 3.1 The HCT and SECT of large and small versions listed for real (core) and biophysical avocados' core temperature.

	Weight [g]	HCT [min]	SECT [min]
Large avocado average ± SD (n=7)	255.6 ± 6.6	76 ± 3	214 ± 8
Large biophysical avocado (n=1)	248.2	76	207
Difference to the mean	3.0%	0	3.0%
Small avocado average ± SD (n=7)	171.0 ± 14.1	51 ± 7	141 ± 16
Small biophysical avocado (n=1)	166.4	54	142
Difference to the mean	2.7%	5.9%	0.4%

The presented results show the expected faster cooling for small avocados compared with the large ones (Figure 3.4). When comparing the SECT for real avocado pulp with the core of the large version of the biophysical avocado, the difference was 3.0%. This means the thermal response of the real avocados was captured by the biophysical one. The comparison of HCT and SECT for the small version revealed the differences of 5.9% and 0.4, respectively. (Table 3.1). Furthermore, it can be observed that there was a cooling lag for both biophysical and real avocado cores compared with the biophysical avocado's surface temperature. In the small version, the difference between the biophysical avocado's surface and both core temperatures was smaller than for the large version due to the smaller distance from the surface to the core (Figure 3.4 b,d). The Biot number for smaller versions is lower at the same airflow conditions, by which the cooling is more uniform. Here it becomes clear that the added value of biophysical food is the highest with larger commodities. The more significant variation in size for the small avocados likely led to an increased variation in the individual cooling times (Table 3.1). Besides, for small commodities, the size of the sensor in relation to the food becomes relatively more significant. Furthermore, when placed in the real avocado, differences in the sensor position will have a stronger

impact on the cooling time. Therefore, we conclude that for avocados, the large biophysical prototypes mimicked the real avocados' thermal response better than the small version, and it is also more relevant for the larger biophysical food.

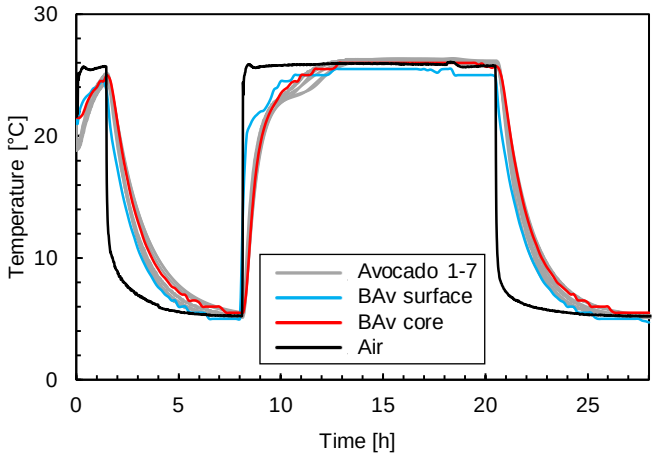

Figure 3.5 Temperature change measured for large biophysical avocado (BAv) and similar-sized real avocados (n=7) in continuous cooling and heating process in two chambers with constant temperatures at 25°C and 5°C, respectively. Monitored temperatures: BAv surface (blue), BAv core (red), pulp of 7 real avocados (grey), and ambient air temperature (black).

In a second experiment, we tested during continuous cooling and heating the temperature change of the large biophysical and similar-sized real avocados (Figure 3.5). It can be seen that the air temperature deviated from the avocado's actual temperature in the cooling and heating stages, but the biophysical avocado's temperature is in line with it. This result underlines the importance of measuring not only air temperature in a real supply chain, which is not representative of the commodities' temperature. In summary, our large biophysical avocado thermal-physically performed well to real avocados.

3.3.2 Potato

Similar to the biophysical avocado, we obtained cooling curves for the biophysical potato (Figure 3.6 a,b) and determined the HCT and SECT for small and large potatoes and their corresponding biophysical potatoes (Table 3.2, Figure 3.6 c,d).

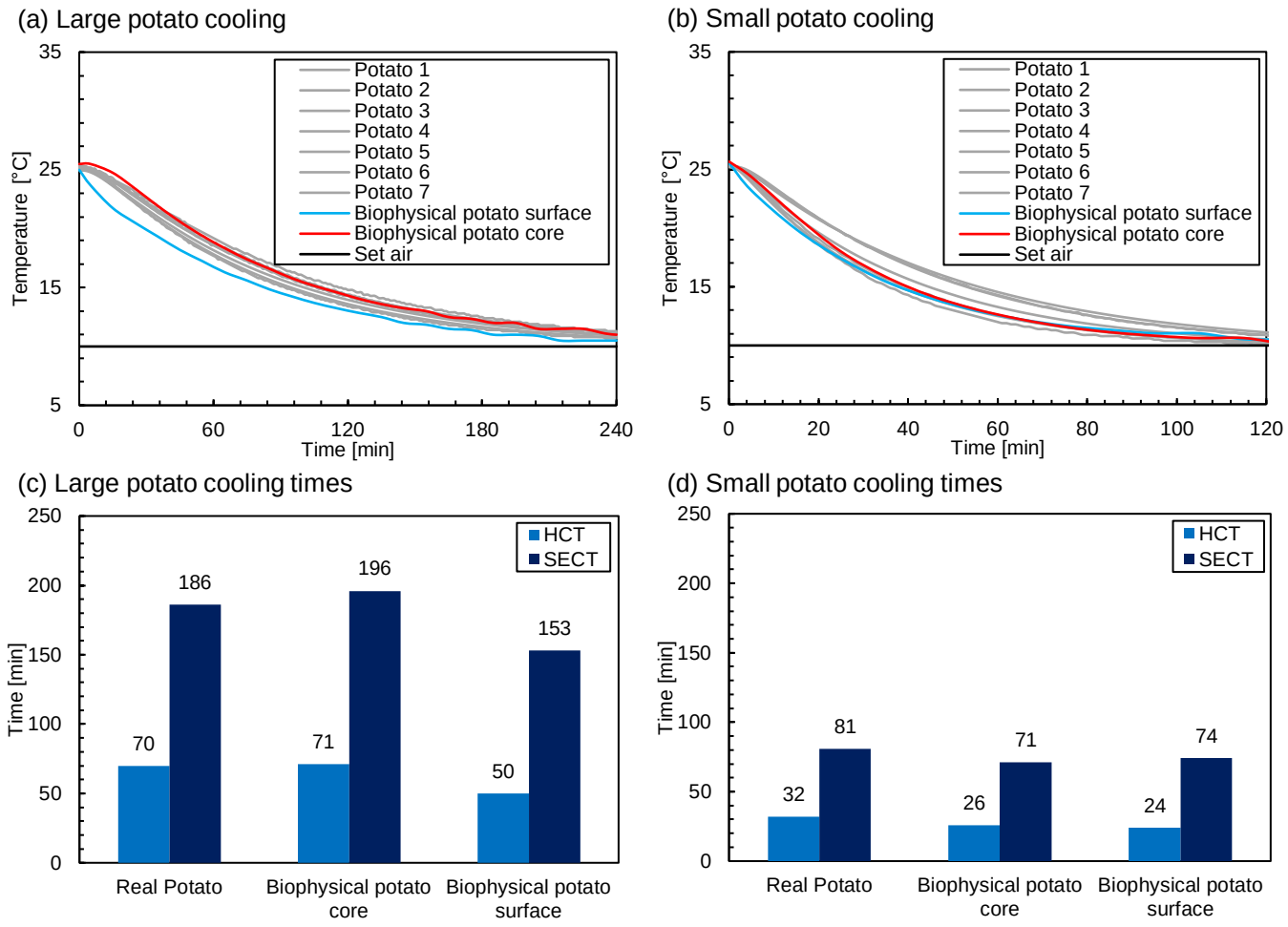

Figure 3.6 Time-dependent temperature change during cooling measured for (a) large and (b) small biophysical and real potatoes. The temperature was monitored for the biophysical potato surface (blue), biophysical potato core (red), and core of the real avocados (grey), whereas chamber set temperature is indicated (black). The HCT and SECT of (c) large and (d) small versions for both real (n=7) and biophysical potatoes (n=1) when cooling from 25°C to 10°C.

Table 3.2 The HCT and SECT of large and small versions listed for real and biophysical potatoes' core temperature.

	Weight [g]	HCT [min]	SECT [min]
Large potato average ± SD (n=7)	231.1 ± 18.7	70 ± 6	186 ± 13
Large biophysical potato (n=1)	215.6	71	196
Difference to the mean	6.7%	1.4%	5.4%
Small potato average ± SD (n=7)	44.4 ± 3.8	32 ± 6	81 ± 14
Small biophysical potato (n=1)	42.9	26	71
Difference to the mean	3.4%	18.8%	12.3%

The results for the large biophysical potato showed a consistent cooling time compared to the real potatoes, with an HCT difference of 1.4% and a SECT difference of 5.4%. Therefore, we conclude that the large biophysical potato captured the thermal responses of real large potatoes (Figure 3.6 a,c). On the other hand, it can be observed that for small biophysical potatoes, both the HCT and SECT had a considerable difference compared to real potatoes, even though the weight difference was smaller than for the large version (Figure 3.6 b,d, Table 3.2). The lower accuracy of the small biophysical potato, reflected by the cooling time, was most likely influenced by the higher measured density difference between the small biophysical potato and the real one (section 3.2). Similarly to avocado, there was a delay in the core temperature compared with surface temperature for the large potatoes (Figure 3.6 a). However, this difference was insignificant in the small version, for which the biophysical potato's surface cooled even slightly slower than the core, which is suboptimal. This result tells us that the temperature gradient from surface to core can be neglected for samples that have very small sizes, so at smaller Biot numbers. In other words, when cooling small commodities, homogeneous temperatures are faster achieved. Thus, similarly to the biophysical avocado, for the biophysical potato, we conclude that prototypes manufactured for larger species or cultivars represent the cooling behavior more accurately and have more practical meaning than that for small versions.

3.4 Biophysical apple deployment in Himachal Pradesh, India

Himachal Pradesh is one of India's largest apple-producing states. We partnered with Coolcrop to deploy our biophysical twin for apples. It was used to monitor temperature from different locations in the cold storage unit. This implementation was also performed to collect feedback for possible improvement in the application from users in an actual cold chain. Monitoring data is presented for two different time points during the storage, namely during the harvesting phase, where the cool room was opened and closed frequently, and new (warm) cargo was added (Figure 3.7 a), and later when the storage was entirely filled with apple and properly cooled down (Figure 3.7 b).

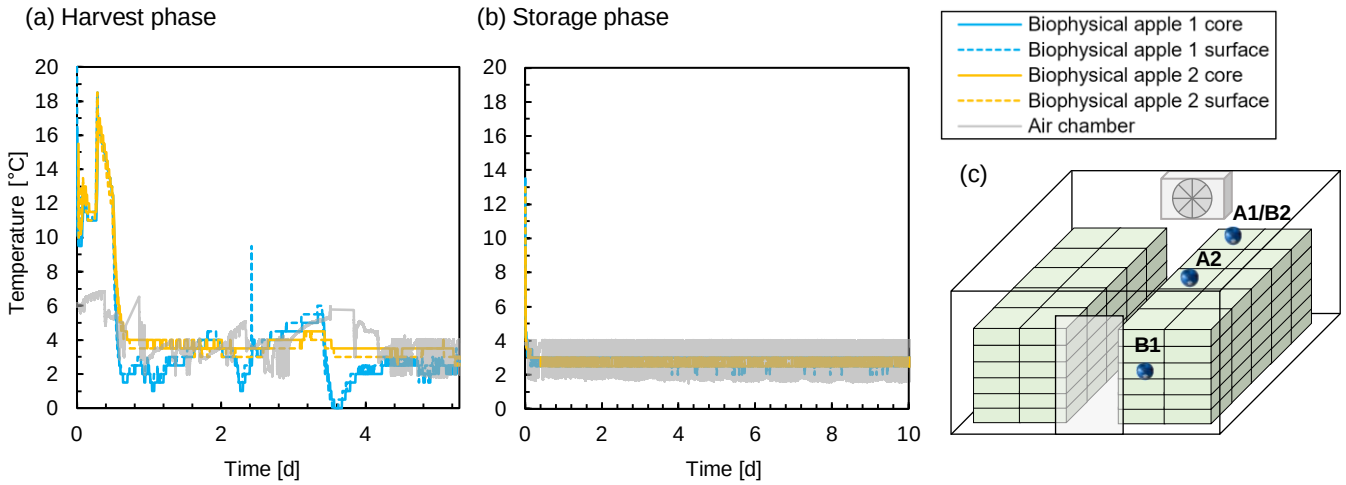

Figure 3.7. Temperature monitoring with biophysical apples in different spots in a cooling chamber. (a) Harvest phase with biophysical apple on crate top: near the evaporator (A1, blue) and near the room center (A2, yellow); (b) Storage phase with biophysical apple in the middle crate at the opposite end of the evaporator near the door (B1, blue) and in the top crate near the evaporator (B2, yellow). The temperature was monitored for ambient air (grey); (c) Schematic drawing set up including biophysical apple position for both of the monitoring experiments.

From the temperature curves shown in Figure 3.7 a, we can observe fluctuations in the chamber air temperature. These can be caused by opening the door or adding newly harvested apples that were still warm. For the biophysical apple 1, which was put near the evaporator where the airflow was fluctuating, the monitored temperature also showed more variation. Interestingly, the temperature of biophysical apple 1 deviated from the measured chamber air temperature. A reason for this could be the position close to the evaporator and its initiated temperature reduction due to increased chamber air temperature (e.g., by the addition of new apples). On the other hand, for the biophysical apple 2 located in the center of the room on top of apples, where the airspeed was low, the measured temperature was consequently more constant. This comparison shows the temperature heterogeneities in a cooling chamber and that applying only one sensor during this initial storage phase could be risky. For example, at around day 3.5, the temperature of biophysical apple 1 dropped to 0°C, which in the long term could lead to chilling injury symptoms depending on the chilling-injury resistance of the apple cultivar. If we only monitor the chamber's air temperature, such temperature variation and possible quality reduction of the apples stored at this location could not be detected. Consequently, we can map temperature differences of storage locations and related risks for too high or too low temperatures by using several biophysical prototypes in a cooling unit. Often cold store providers or operators do not have a clear view of the temperature heterogeneity in their cold stores, especially when placing new (warm) cargo inside. By the biophysical food information, not only adequate storage operations can be initiated, but also more information on the product temperature-related quality is gained.

In Figure 3.7 b, it can be seen that homogenous cooling was present at all monitored locations later in the storage period. During this time, the stored volume of apples was constant, and possibly the storage unit was not opened regularly. Therefore, we conclude that biophysical food is more useful during the initial storage phase when products are cooled down and added in batches at different times. Also, in the long-term storage phase, where all food is conditioned, biophysical food at different locations gives less additional temperature insights. Apples are often stored for prolonged periods, but several other fresh produce never has such prolonged storage duration, especially when intended for the domestic market.

Finally, we also received feedback from the operators regarding the application of the biophysical apples. One concern was that the surface sensors sometimes detached during usage since the double-sided adhesive pads were not strong enough to fix them tightly. In the future, a better substitute to stick the sensors to the biophysical food will be implemented. Also, the wish for an automatic readout instead of a USB readout from the current iButtons was raised. A data extraction through a mobile phone that is more accessible and portable could be an option. This method would accelerate the data retrieval process and increase the working efficiency.

3.5 Outlook

The biophysical food in this study has not been commercialized. Compared to products already on the market, some limitations still need to be solved. For example, the ImpacTrack includes a temperature sensor and a shock sensor to identify risks for bruise

damages (MartinLishman, 2022). Furthermore, this product serves the advantage that the logger has a wireless readout and can directly be connected to a mobile phone via Bluetooth. Besides, it is available for various commodities, including pear, peach, and corn. Another example is the SolAntenna, a simulator for potato products also providing automated real-time information (Pessl instruments, 2022). Additionally, it measures parameters including CO_2, temperature, and relative humidity and has a wireless readout. On the other hand, both aforementioned companies declare that their products mimic real commodities' weight and density. However, it did not declare in detail how this was achieved. Since these products are made of only a plastic shell, their thermal response could deviate from the real commodities. Our study showed that the filling of a biophysical food needs to be adjusted for each fresh produce to mimic its thermal response realistically. By this, we present the unique characteristic of the developed biophysical food. Nevertheless, to accelerate and upscale the product development for commercialization, the manufacturing protocol could be further simplified, which could be investigated in future research.

Other possible upgrades of our current biophysical food models could be implementing an alternative sensor-log device for direct connection and wireless readout via mobile phone or computer. The option for real-time monitoring would benefit, as stakeholders could directly see what is happening in the cold chains to take the proper actions. In the ideal case, the logger device could also include other relevant sensors (e.g., respiratory gases or air speed) (Geyer et al., 2018; Keshri et al., 2020). Note that in the current version, additionally to temperature, humidity can be measured by using a Hygrochron (DS1923) instead of a Thermochron (DS1921G and DS1922L) iButton at the surface. However, this sensor will considerably increase the total costs of biophysical food. Thus, considering cost and accuracy, it is challenging to realize that an affordable multisensory device additionally has a long battery lifetime (Cho et al., 2005; Clements et al., 1998; Dickert, Hayden, & Zenkel, 1999).

4 CONCLUSIONS

We aimed to bring the use of biophysical food in supply chains closer to implementation in this study. We successfully optimized the existing biophysical food for apples by optimizing the manufacturing process to scale up straightforwardly, adjusting the pH of the filling to inhibit fungal growth, adding unique color, and applying a food-grade coating. Furthermore, we deployed biophysical apple prototypes in the apple value chain of Himachal Pradesh, India, to better understand the cooling process in a storage unit. Second, we developed new biophysical food for avocado and potato, in both large and small sizes. We found that the large prototypes more accurately captured the cooling behavior of the pulp temperature. A clear temperature gradient between the surface and core was detected in the avocado or potato during the cooling process. Small biophysical prototypes are not practical due to larger differences in cooling behavior compared to real commodities and similar surface and core temperatures. The added value of the biophysical food is thereby higher for larger products. Biophysical food for different products can be applied in individual operations or entire supply chains. By installing them in multi-locations, we identified high-risk storage spots where the most significant temperature heterogeneities occur. Besides preserving the food longer by cold storage, the biophysical food data will help avoid chilling injury or temperature-induced microbial growth.

Acknowledgments

This work was partially funded by the data.org Inclusive Growth and Recovery Challenge grant "Your Virtual Cold Chain Assistant", supported by The Rockefeller Foundation and the Mastercard Center for Inclusive Growth. The funder was not involved in the study design, collection, analysis, interpretation of data, the writing of this article, or the decision to submit it for publication. The authors would like to thank Srinivas K. Marella, Ajay Sharma, Karan Dass, and Kendall Nowocin of Coolcrop Technologies Pvt. Ltd. (India) for the collaboration, data collection, and application feedback. This manuscript has been released as a preprint on engrXiv.

Author Contributions

T.D. conceptualized the study and acquired funding; T.D. did the project administration; L.Y. and S.S. performed the investigation, developed the methodology; L.Y. executed the experiments with key inputs from T.D. and S.S.; L.Y. wrote the original draft of the paper and did the visualization; S.S. and T.D. and performed critical review and editing.

REFERENCES

Ahangarnezhad, N., Najafi, G., & Jahanbakhshi, A. (2019). Determination of the physical and mechanical properties of a potato (the Agria variety) in order to mechanise the harvesting and post-harvesting operations. *Research in Agricultural Engineering*, *65*(2), 33–39.

ASHRAE Research. (2018). *ASHRAE Handbook: Refrigeration* (SI Edition). Amer Society of Heating.

Cho, J.-H., Yu, J.-B., Kim, J.-S., Sohn, S.-O., Lee, D.-D., & Huh, J.-S. (2005). Sensing behaviors of polypyrrole sensor under humidity condition. *Sensors and Actuators B: Chemical*, *108*(1), 389–392. https://doi.org/https://doi.org/10.1016/j.snb.2004.12.082

Clark, C. J., White, A., Jordan, R. B., & Woolf, A. B. (2007). Challenges associated with segregation of avocados of differing maturity using density sorting at harvest. *Postharvest Biology and Technology*, *46*(2), 119–127.

Clements, J., Boden, N., Gibson, T. D., Chandler, R. C., Hulbert, J. N., & Ruck-Keene, E. A. (1998). Novel, self-organising materials for use in gas sensor arrays: beating the humidity problem. *Sensors and Actuators B: Chemical*, *47*(1–3), 37–42.

de Mello Vasconcelos, O. C., de Campos Ferreira, G. J. B., de Castro Silva, J., Teruel Mederos, B. J., & de Freitas, S. T. (2019). Development of an artificial fruit prototype for monitoring mango skin and flesh temperatures during storage and transportation. *Postharvest Biology and Technology*, *158*(July). https://doi.org/10.1016/j.postharvbio.2019.110956

Defraeye, T., Tagliavini, G., Wu, W., Prawiranto, K., Schudel, S., Assefa Kerisima, M., … Bühlmann, A. (2019). Digital twins probe into food cooling and biochemical quality changes for reducing losses in refrigerated supply chains. *Resources, Conservation and Recycling*, *149*, 778–794. https://doi.org/10.1016/j.resconrec.2019.06.002

Defraeye, T., Wu, W., Prawiranto, K., Fortunato, G., Kemp, S., Hartmann, S., … Nicolai, B. (2017). Artificial fruit for monitoring the thermal history of horticultural produce in the cold chain. *Journal of Food Engineering*, *215*, 51–60. https://doi.org/10.1016/j.jfoodeng.2017.07.012

Dickert, F. L., Hayden, O., & Zenkel, M. E. (1999). Detection of volatile compounds with mass-sensitive sensor arrays in the presence of variable ambient humidity. *Analytical Chemistry*, *71*(7), 1338–1341.

Dixon, J., Smith, D. B., Elmsly, T. A., Industry, A., & Box, P. O. (2004). Fruit Age , Storage Temperature and Maturity Effects on Hass Avocado Fruit Quality and Ripening. *New Zealand Avocado Growers Association Annual Research Report*, *4*, 47–53.

Dreher, M. L., & Davenport, A. J. (2013). Hass avocado composition and potential health effects. *Critical Reviews in Food Science and Nutrition*, *53*(7), 738–750.

Ejiofor, N. C., Ezeagu, I. E., Ayoola, M., & Umera, E. A. (2018). Determination of the chemical composition of avocado (Persea americana) seed. *Adv Food Technol Nutr Sci Open J*.

Fang, S. W., Li, C. F., & Shih, D. Y. C. (1994). Anti-fungal Activity of Chitosan and Its Preservative Effect on Low-Sugar Candied Kumquat. *Journal of Food Protection*, *57*(2), 136–140. https://doi.org/10.4315/0362-028X-57.2.136

FAO. (2008). Potatoes, nutrition and diet. Retrieved October 12, 2021, from https://www.fao.org/potato-2008/en/potato/factsheets.html

FAO. (2013). *Food Wastage Footprint Impacts on natural resources. Technical Report*. 249. Retrieved from https://www.fao.org/3/i3347e/i3347e.pdf

FAO. (2015). Infographics Food loss and waste facts. Retrieved October 12, 2021, from https://www.fao.org/save-food/resources/

Ferrándiz-Mas, V., & García-Alcocel, E. (2013). Durability of expanded polystyrene mortars. *Construction and Building Materials*, *46*, 175–182.

Geyer, M., Praeger, U., Truppel, I., Scaar, H., Neuwald, D. A., Jedermann, R., & Gottschalk, K. (2018). *Measuring Device for Air Speed in Macroporous Media and Its Application Inside Apple Storage Bins*. https://doi.org/10.3390/s18020576

Hajduković, M., Knez, N., Knez, F., & Kolšek, J. (2017). Fire performance of external thermal insulation composite system (ETICS) facades with expanded polystyrene (EPS) insulation and thin rendering. *Fire Technology*, *53*(1), 173–209.

Hassan, R. A., Sand, M. I., & El-Kadi, S. M. (2012). Effect of some organic acids on fungal growth and their toxins production. *Journal of Agricultural Chemistry and Biotechnology*, *3*(9), 391–397. https://doi.org/10.21608/jacb.2012.55011

Hübert, T., & Lang, C. (2012). Artificial fruit: postharvest online monitoring of agricultural food by measuring humidity and temperature. *International Journal of Thermophysics*, *33*(8), 1606–1615.

Kader, A. A., & Yahia, E. M. (2011). Postharvest biology of tropical and subtropical fruits. In *Postharvest Biology and Technology of Tropical and Subtropical Fruits* (Vol. 1). https://doi.org/10.1533/9780857093622.79

Keshri, N., Truppel, I., Herppich, W. B., Geyer, M., Weltzien, C., & Mahajan, P. V. (2020). In-Situ Measurement of Fresh Produce Respiration Using a Modular Sensor-Based System. *Sensors (Basel, Switzerland)*, *20*(12), 3589. https://doi.org/10.3390/s20123589

Kumar, A., & Singh, G. (2020). Effect of foliar application of bio-stimulants on apple cv. royal delicious. *Plant Archives*, *20*(1), 891–894.

MartinLishman. (2022). ImpacTrack. Retrieved February 10, 2022, from https://martinlishman.com/impactrack/

Mpelasoka, B. S., Behboudian, M. H., & Ganesh, S. (2001). Fruit quality attributes and their interrelationships of “Braeburn” apple in response to deficit irrigation and to crop load. *Gartenbauwissenschaft*, *66*(5), 247–253.

Olaeta, J. A., Schwartz, M., Undurraga, P., & Contreas, S. (2007). Use of Hass avocado (Persea americana Mill) seed as a processed product. *Proceedings of the VI World Avocado Congress*, *20*, 1–8.

Onwude, D. I., Chen, G., Eke-Emezie, N., Kabutey, A., Khaled, A. Y., & Sturm, B. (2020). Recent advances in reducing food losses in the supply chain of fresh agricultural produce. *Processes*, *8*(11), 1431.

Pennington, J. A. T., & Fisher, R. A. (2010). Food component profiles for fruit and vegetable subgroups. *Journal of Food Composition and Analysis*, *23*(5), 411–418. https://doi.org/https://doi.org/10.1016/j.jfca.2010.01.008

Pessl instruments. (2022). SolAntenna. Retrieved February 10, 2022, from https://metos.at/solantenna/

Puttongsiri, T., Choosakul, N., & Sakulwilaingam, D. (2012). Moisture content and physical properties of instant mashed potato. *International Conference on Nutrition and Food Science*, *39*, 92–95.

Ramezani, R., & Aminlari, M. (2004). Comparing chemical composition of four potato varieties for processing. *Journal of Food Science and Technology - Mysore*, *41*(6), 689–691.

Rousk, J., Bååth, E., Brookes, P. C., Lauber, C. L., Lozupone, C., Caporaso, J. G., … Fierer, N. (2010). Soil bacterial and fungal communities across a pH gradient in an arable soil. *The ISME Journal*, *4*(10), 1340–1351. https://doi.org/10.1038/ismej.2010.58

Salazar-López, N. J., Domínguez-Avila, J. A., Yahia, E. M., Belmonte-Herrera, B. H., Wall-Medrano, A., Montalvo-González, E., & González-Aguilar, G. A. (2020). Avocado fruit and by-products as potential sources of bioactive compounds. *Food Research International*, *138*, 109774.

Shoji, K., Schudel, S., Onwude, D., Shrivastava, C., & Defraeye, T. (2022). Mapping the postharvest life of imported fruits from packhouse to retail stores using physics-based digital twins. *Resources, Conservation and Recycling*, *176*, 105914. https://doi.org/10.1016/j.resconrec.2021.105914

Shokri, H. (2011). Evaluation of inhibitory effects of citric and tartaric acids and their combination on the growth of Trichophyton mentagrophytes, Aspergillus fumigatus, Candida albicans, and Malassezia furfur. *Comparative Clinical Pathology*, *20*(5), 543–545. https://doi.org/10.1007/s00580-011-1195-6

Singh, D. K., Goswamin, T. K., & Chourasia, M. K. (2006). Physical properties of two popular indian potato varieties. *Journal of Food Process Engineering*, *29*(4), 337–348. https://doi.org/10.1111/j.1745-4530.2006.00066.x

Singh, F., Katiyar, V. K., & Singh, B. P. (2015). Mathematical modeling to study influence of porosity on apple and potato during dehydration. *Journal of Food Science and Technology*, *52*(9), 5442–5455.

Sukhpreet, K., & Poonam, A. (2014). Studies on Indian potato genotypes for their processing and nutritional quality attributes. *International Journal of Current Microbiology and Applied Sciences*, *3*(8), 172–177.

Valente, M., Chambarel, A., Cordonnier, J., & Pumborios, M. (1996). Finite element modelling of heat transfer in avocados. *International Agrophysics*, *10*(2), 123–129.

Wu, W., & Defraeye, T. (2018). Identifying heterogeneities in cooling and quality evolution for a pallet of packed fresh fruit by using virtual cold chains. *Applied Thermal Engineering*, *133*, 407–417. https://doi.org/https://doi.org/10.1016/j.applthermaleng.2017.11.049

Yang, Y., Achaerandio, I., & Pujolà, M. (2016). Classification of potato cultivars to establish their processing aptitude. *Journal of the Science of Food and Agriculture*, *96*(2), 413–421.

APPENDIX

Table A. 1 Measured dimension and density of small and large avocado

	Small avocado (n=30)	Large avocado (n=5)
Length avocado [mm]	79.76 ± 6.35	97.95 ± 5.72
Width avocado [mm]	58.90 ± 2.34	70.64 ± 1.26
Length seed [mm]	31.42 ± 2.83	42.70 ± 7.43
Width seed [mm]	28.20 ± 5.26	36.32 ± 4.40
Density avocado [g/cm^3]	1.02 ± 0.02	0.98 ± 0.01
Density seed [g/cm^3]	1.18 ± 0.23	1.18 ± 0.07
Density pulp [g/cm^3]	1.00 ± 0.02	0.96 ± 0.01

Table A. 2 Dimension and density of the small and large potato

	Small potato (n=30) (D. K. Singh et al., 2006)	Large potato (n=100) (Ahangarnezhad et al., 2019)
Length potato [mm]	57.68 ± 16.37	91.23 ± 18.16
Width potato [mm]	37.77 ± 6.01	63.17 ± 12.96
Density potato [g/cm^3]	1.11 ± 0.02	1.05 ± 0.14